Modular High Field Quadrupole Design for Electron–Ion Collider

Ramesh Gupta, Michael Anerella, John Cozzolino, Brett Parker, Shailendra Chouhan, Stephen Kahn, James Kolonko, Delbert Larson, Ron Scanlan, Robert J. Weggel, and Erich Willen

***Abstract*—The proposed electron–ion collider (EIC) needs high-gradient, large-aperture quadrupole magnets in the interaction region (IR). This paper presents the work under a Small Business Innovation Research Phase I grant to Particle Beam Lasers, Inc., and Brookhaven National Laboratory (BNL) to develop a novel modular design for EIC quadrupoles based on racetrack coils, which need no expensive tooling to build. It also enables the same coils to be used in Nb_3Sn magnets of a range of apertures. Such a modular program may greatly facilitate R&D and reduce its costs, which often dominate the total cost of magnets that are one-of-a-kind or produced in limited numbers. For the EIC IR, the same coils are used in four R&D quadrupoles: one Nb_3Sn quadrupole as proposed for the BNL eRHIC and three Nb_3Sn quadrupoles as proposed by Jefferson Laboratory for JLEIC. This paper will present the basic magnetic and mechanical design of the several IR quadrupoles for the proposed EIC.**

***Index Terms*—High gradient quadrupoles, Nb_3Sn quadrupoles, racetrack coil quadrupoles, modular magnet design, Electron Ion Collider, EIC.**

I. Introduction

THE proposed Electron-Ion Collider (EIC) could unravel the mysteries of the atomic nucleus by using high energy electron beams colliding with ion or proton beams [1]. One of the key elements in the proposal is the Interaction Region (IR) quadrupoles. The present designs of the EIC quadrupoles, and of most superconducting quadrupoles in accelerator and beam line magnets, are based on the $\cos(2\theta)$ design, which is efficient in creating field gradient. However, the high pole field required of the EIC quadrupoles necessitates the use of Nb_3Sn, which is less robust and much less forgiving of strain than NiTi. A Nb_3Sn quadrupole is likely to be more reliable and less likely to quench if all of its windings are planar racetracks, rather than non-planar and complex windings, as in the $\cos(2\theta)$ design, with its compound-curvature ends. This PBL/BNL SBIR is to develop high pole field quadrupole designs for the EIC based on simple racetrack coils proposed earlier for the upgrade of Large Hadron Collider [2].

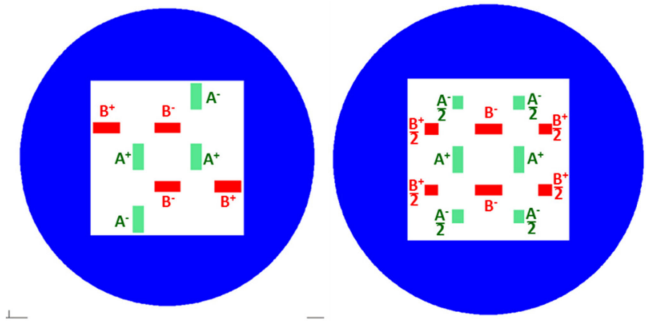

Fig. 1. Two versions of the modular quadrupole designs. The one on the left is simpler and uses four sets of racetrack coils; the one on the right is symmetric and uses eight sets of racetrack coils.

The coil configuration close to the bore resembles a Panofsky quadrupole [3]. Near the magnet midplane the conductor, which generates most of the field gradient in the modular design, is at the same radius as in the $\cos(2\theta)$ design. This is significantly different from the other racetrack coil geometries examined earlier [4], [5]. Therefore, as explained in [2], the efficiency of that part of the magnet resembles that of the $\cos(2\theta)$ designs in creating the field gradient, even though the amount of conductor used per magnet will be over a factor of two larger.

The modular design facilitates an R&D approach that is particularly cost-effective and suitable when only a few quadrupoles with different apertures are needed. In a large production, the cost of material and labor play a much bigger role than the cost of R&D, engineering and design. However, for a small production like that needed for the EIC, the cost of material (such as the cost of superconductor) is a relatively smaller fraction of the overall cost of the project. In such cases a better figure of merit may be the ability of conductor to create the field gradient rather than the amount of conductor used. Reduction in margin due to inherently better performing designs is another figure of merit. The design and technical approach presented here makes racetrack coils more attractive for a variety of high gradient quadrupole applications such as in an Electron Ion Collider.

II. Modular Design Concept

Figure 1 pictures two modular quadrupole design configurations: (a) A *"simpler design"* (left), in which it is extraordinarily

Manuscript received October 30, 2018; accepted January 14, 2019. Date of publication February 6, 2019; date of current version February 14, 2019. This work was supported in part by Brookhaven Science Associates, LLC, under Contract DE-SC0012704 and in part by the U.S. Department of Energy SBIR under Grant DE-SC0018615 to Particle Beam Lasers, Inc. *(Corresponding author: Ramesh Gupta.)*

R. Gupta, M. Anerella, J. Cozzolino, and B. Parker are with Brookhaven National Laboratory, Upton, NY 11973 USA (e-mail: gupta@bnl.gov).

S. Chouhan, S. Kahn, J. Kolonko, D. Larson, R. Scanlan, R. J. Weggel, and E. Willen are with Particle Beam Lasers, Inc., Northridge, CA 91324-2807 USA.

Color versions of one or more of the figures in this paper are available online at http://ieeexplore.ieee.org.

Digital Object Identifier 10.1109/TASC.2019.2896376

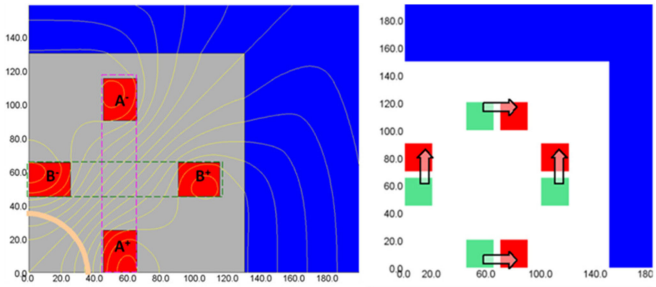

Fig. 2. Modular designs offer a valuable R&D opportunity to increase the magnet aperture from the figure at the left to that at the right by moving racetrack coil *A* to the right and coil *B* upwards by the same amount.

TABLE I
KEY DESIGN PARAMETERS OF Nb_3Sn QUADRUPOLES FOR THE EIC IR

	Q1PF	QFFB1_US	QFFB2_US	QFFB3_US
EIC Design	BNL	JLab	JLab	JLab
Aperture (mm)	96	60	80	80
Field Gradient (T/m)	140	141	149	116
Magnetic Length (m)	1.5	1.2	1.5	1.0

simple to assemble coils into a magnet and (b) a *"symmetric design"* (right), which maintains the mirror symmetry typical of quadrupole magnets. These designs employ a set of simple racetrack coils (A and B) placed in a quadrupole configuration such that the conductor at the mid-plane, which contributes most to the field, is placed at the minimum coil radius. We refer to these designs as "Modular Designs" because the quadrupole coils are made of simple racetrack "modules". Several such coil modules can be stacked, and an individual coil module can be replaced to carry out a fast-turn-around, low cost and systematic quadrupole magnet R&D program. Most of the gradient is generated by blocks A+ and B−, with return blocks A− and B+ (or A−/2 and B+/2) adding marginally. In the symmetric design, the coils in two quadrants need to clear each other in the end region (a complication). This is not a problem in the simpler design.

The modular designs also offer a unique opportunity to change the quadrupole apertures while using the same coil modules, particularly for an R&D program. Figure 2 demonstrates the first-quadrant coil translations to increase the aperture of the *simpler* magnet of Fig. 1 (left) by moving coil A^+/A^- to the right and coil B^+/B^- upwards by the same amount.

III. MAGNETIC DESIGN ANALYSIS

We will carry out the magnetic design calculations for the following for EIC quadrupoles [6]–[9] which require the use of Nb_3Sn coils: (a) BNL Q1PF, (b) JLab QFFB1_US, (c) JLab QFFB2_US, (d) JLab QFFB3_US. The design parameters of these magnets are still evolving; the parameters used in this study are shown in Table I. Even though the initial design optimization has been carried out for Q1PF, it will be shown in at least one case that the same racetrack coil cross-section can be used as well in other quadrupoles with differences in field gradient, aperture and other design parameters. The modular design is expected to

TABLE II
BASIC CONDUCTOR PARAMETERS

Strand Diameter (mm)	0.8
Cu to non-cu ratio	1.17
Number of strands	35
Cable insulation (mm)	0.1
Cable width, bare (mm)	15.15
Mid-thickness (mm)	1.338
Keystone angle	0.75
Cable width, insulated (mm)	15.35
Mid-thickness, insulated (mm)	1.637
Cable I_c (4.4K, 13.54 T), A/mm^2	2087

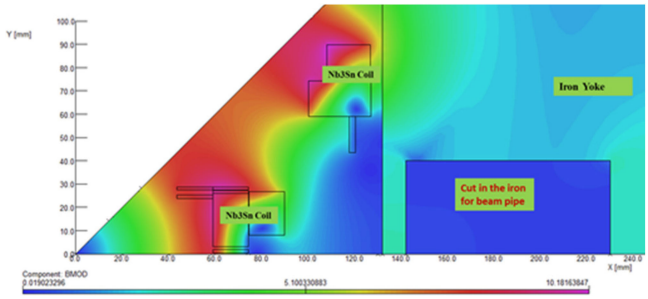

Fig. 3. OPERA2d model of an octant of the symmetric modular design *"A"* with two layers of coils, in addition to a turn pole block. Return coil blocks are further away from the aperture. The blue rectangle is a cutout in the yoke for the electron beam.

reduce the project costs of the EIC by minimizing the R&D and tooling costs required for each magnet, particularly when only one of each kind is needed.

Another design requirement which is specific to these EIC quadrupoles is the need for a nearly field-free region for the close-by electron beam in the interaction region [IR]. As discussed in another paper [10], we propose to use passive shielding to isolate the electron beam from the fields that bend or focus the ion beam.

All designs to be presented in this paper will utilize the same Nb_3Sn cable with parameters used in the LARP quadrupole [11]. Table II lists these parameters.

A. Magnet Cross-Section Design

We present optimized cross-sections of several configurations, all using the same cable. They are shown in Figs. 3-6 below and summarized in Table III. The design field gradient for Q1PF is 140 T/m, and the coil aperture is 96 mm. The first two designs (Fig. 3 and Fig. 4) have two layers of coils, and the last two (Fig. 5 and Fig. 6) have one layer. The first design (Fig. 3) has small 2-turn pole coils. The first three designs (Figs. 3-5) are *symmetric,* and the fourth one (Fig. 6) is *simpler.* In addition to the normal allowed harmonics, the simpler design can have certain allowed skew harmonics which are optimized to become negligible.

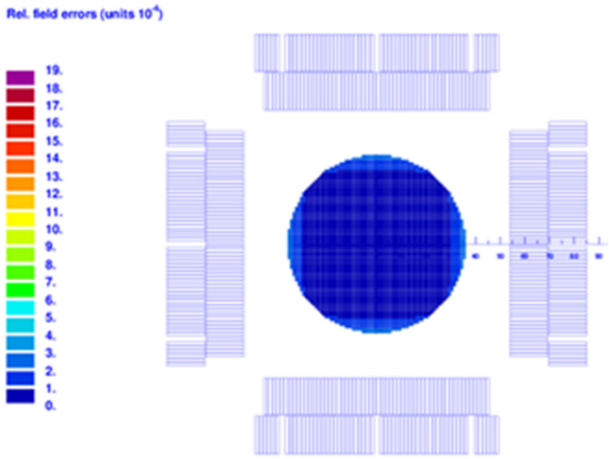

Fig. 4. Optimized ROXIE model of the main coil blocks of the symmetric 2-layer modular design *B*, which does not require extra pole blocks. Return coil blocks and yoke iron (not shown here) are included in the calculations.

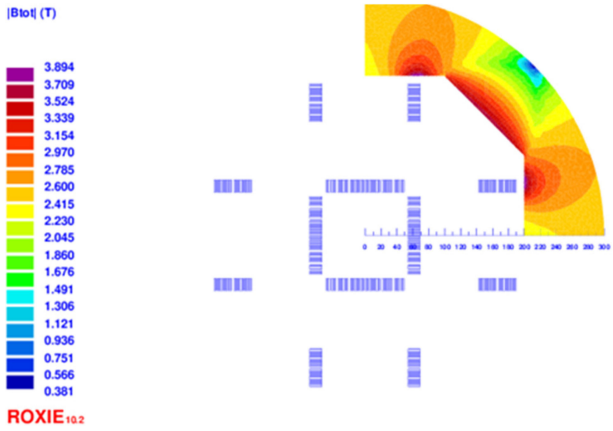

Fig. 5. Optimized ROXIE model of the main coil blocks and return coil and quadrant of the iron yoke of the symmetric 1-layer modular design *C*. The outer radius of iron is 300 mm.

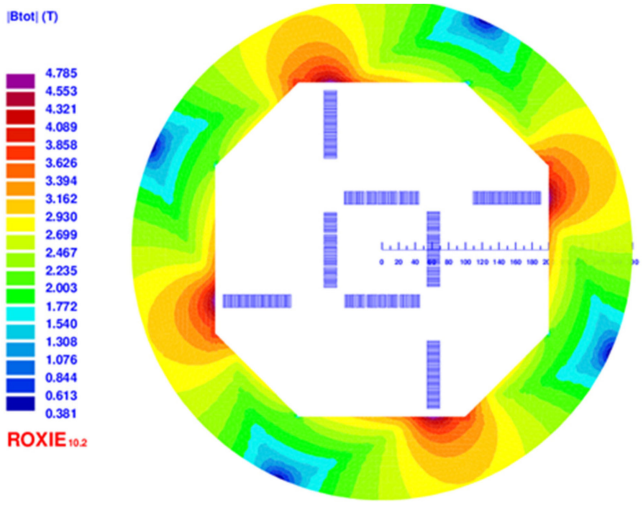

Fig. 6. Optimized ROXIE model of the main coil blocks, return coil and the iron yoke of the simpler 1-layer modular design *D*, which facilitates assembly of the coils into a magnet but lacks mirror symmetry, thereby introducing skew harmonics. We were able to keep them small (<1 unit) in optimization. The magnet needs to be installed with a rotation of about 7.5 degree to avoid the skew quadrupole.

TABLE III
MODULAR DESIGNS OF 96 MM BORE Q1PF WITH A GRADIENT OF 140 T/M

	Design A	Design B	Design C	Design D*
Symmetric or Simpler	Symm	Symm	Symm	Simp
Number of Layers	2	2	1	1
Additional Pole block	Yes	No	No	No
Number of turns	68	56	27	25
Operating Current, A	12880	9,008	17,000	17,073
% on the Loadline	60	62.7	88.2	87.1
b_6 @36 mm	-0.22	-1.15	0.02	-0.03
b_{10} @36 mm	-0.95	-1.60	0.00	0.28
b_{14} @36 mm	0.13	0.43	-0.36	-0.02

*Design D only ($a_6 = -0.86$, $a_{10} = -0.15$ and $a_{14} = 0.03$).

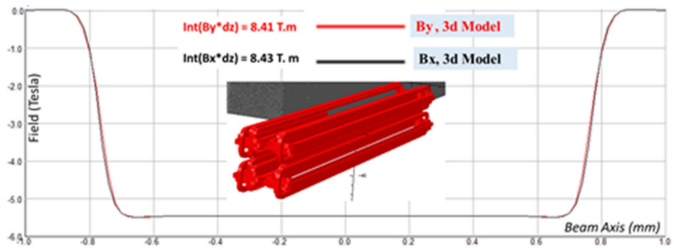

Fig. 7. OPERA3d model with the ends optimized to make field integral along the horizontal and vertical axis nearly the same.

The normal and skew harmonics (b_n and a_n) are defined in the following expression:

$$B_y + iB_x = 10^{-4} \times B_{R0} \sum_{n=1}^{\infty} (b_n + ia_n)[(x+iy)/R]^{n-1},$$

where B_x and B_y are the components of the field at (*x, y*), and B_{R0} is the magnitude of the field due to the most dominant quadrupole harmonic (n = 2) at a reference radius, *R*.

Fig. 3 shows OPERA2d field contour plot of an octant of the symmetric two-layer coil design with an additional pole coil for the quadrupole Q1PF in the BNL design. It also shows part of the iron yoke containing a cutout for the electron beam. We carried out a simulation where we moved the coils of this design to create the aperture for the JLab quadrupoles QFFB1_US, QFFB2_US, QFFB3_US designs and were able to obtain good field quality.

Fig. 7 shows OPERA 3d ends of a symmetric modular design (see inset), with the ends of the coil optimized to nearly equalize the field integral along the horizontal and vertical axes.

IV. MECHANICAL DESIGN ANALYSIS

A structural analysis of both the *simpler* design (design D) and the *symmetric* design (design A) were performed using the ANSYS finite element program. For the analysis we have assumed that coils are held in place with a stainless steel 304 collar that has a 96 mm aperture hole for the beam. The procedure was to use ANSYS to calculate the field (and compare it to OPERA) to obtain the Lorentz forces locally at each node. Because the *simpler* design does not satisfy the normal mirror symmetry, an anti-symmetric 90° rotational boundary condition was used

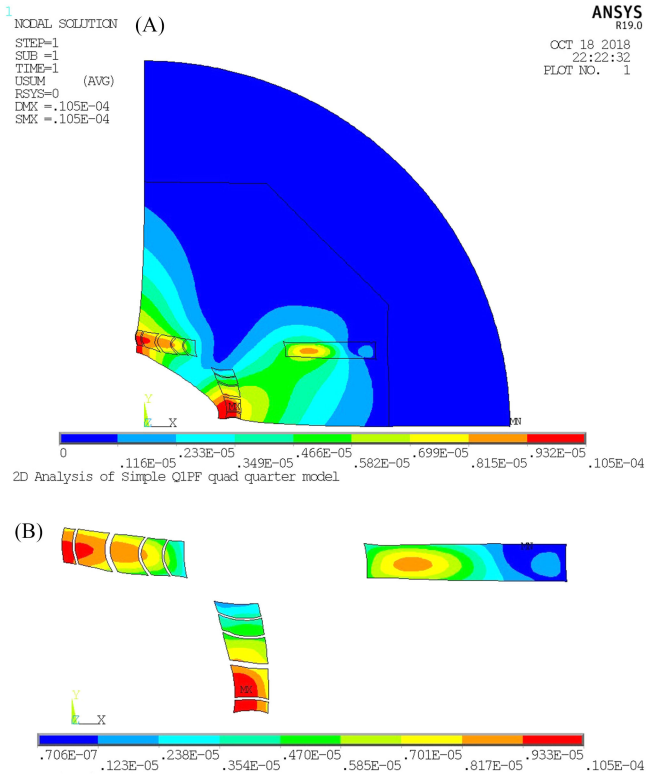

Fig. 8. (a) Contour plot of displacements from the Lorentz forces for the simpler design. (b) Blow up of the displacements in the coils.

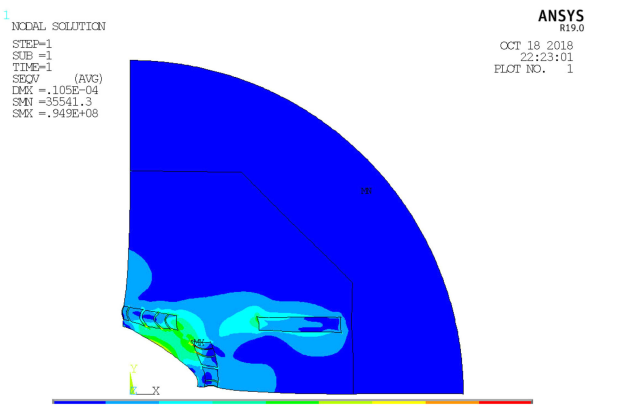

Fig. 9. Von Mises stress from the Lorentz forces for the simpler design.

for the magnetic simulation. (A boundary condition on the vector potential, $A_z(0°) = -A_z(90°)$ was imposed.) Because the Lorentz forces are proportional to both J and B, the mechanical displacements show a 90° rotational symmetry. Fig. 8a shows a contour plot of the nodal displacements of the simpler design model. The maximum displacement observed is 10.5 μm and occurs at the coil mid-planes. Fig. 8b shows an enlarged view of the displacements in the coils.

Fig. 9 shows the von Mises stress for the *simpler* design. The peak stress occurs in the collar between the coils. There is also a bending stress that occurs on the inner surface of the aperture. We have used a Young's modulus of 44 GPa for the Nb_3Sn cable [5] in order to calculate the strain on the conductor from

TABLE IV
KEY PEAK STRUCTURAL VALUES FOR THE DESIGN CONSIDERED

	Simpler	Symmetric	Material Limit
Design	D	A	
Maximum Displacement (μm)	10.5	9.3	
Peak von Mises Stress on Collar (MPa)	95	116	215
Peak von Mises Stress on Coil	46	56	210
Peak Coil Strain	0.1%	0.13%	0.23% to 0.28%

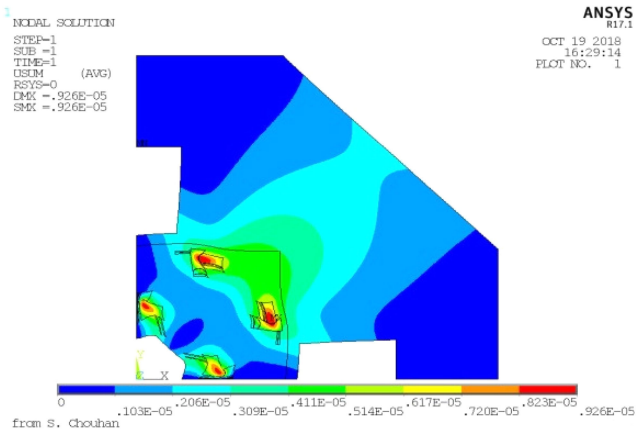

Fig. 10. Contour plot of displacements from the Lorentz forces for the symmetric design A.

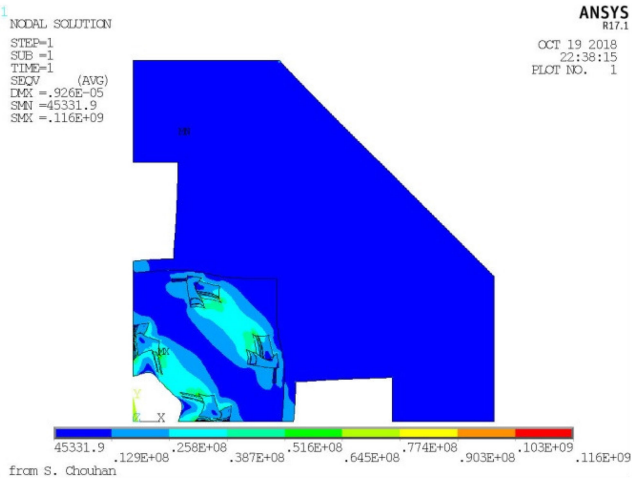

Fig. 11. Contour plot of van Mises stress for the symmetric design A.

the Lorentz forces. Table IV summarizes the peak values for this design in column 2. The limiting material values [5], [11], [12] are shown for comparison. The peak structural values are sufficiently below the limiting material values.

A similar analysis has been performed for the *symmetric* design A. The boundary conditions for this case are simpler. The magnetic field is normal to the mid-plane, and the perpendicular displacement on the mid-plane is zero. Fig. 10 shows the displacement contour plot, which indicates that the maximum displacement occurs at the coils. The maximum displacement is only 9.3 μm, which is quite acceptable. Fig. 11 shows the von

Mises stress for this design. The region with the largest stress is on the collar in the vicinity of the space between the coils. The peak values of displacement, stress and strain for the symmetric design are summarized in Table IV.

V. Conclusion

As a part of the Phase I SBIR, we examined the advantages of the modular quadrupole design for the Electron-Ion Collider. Modular designs are based on racetrack coils, which are less expensive to manufacture; simpler tooling suffices. Modular quadrupoles, as the Panofsky quadrupole, have conductor at the midplane, closer to the aperture, for creating field. Their support structure is simpler, and often they perform more reliably than the cosine theta coils, with their complex end geometry. We also demonstrated that the same racetrack coils can be used to produce field-quality designs of several IR quadrupoles of JLEIC at JLab and Q1PF of eRHIC at BNL. This is a major advantage of the modular design for high gradient quadrupole, where R&D cost dominates the project cost when only one of each kind is needed. Two options of the modular design have been investigated. The *symmetric* design maintains the standard quadrupole mirror symmetry; however, winding such coils is more complex, because the coil ends intersect. The *simpler* design avoids the complications at the coil ends; however, because it breaks the quadrupole mirror symmetry, it potentially allows undesired skew harmonics. It is shown that higher order harmonics can be removed during optimization, and first order (skew quadrupole) during installation. A proof-of-principle magnet will be built during Phase II, if funded.

References

[1] National Academies of Sciences, Engineering, and Medicine, *An Assessment of U.S.-Based Electron-Ion Collider Science*. Washington, DC, USA: Nat. Academies Press, 2018.

[2] R. Gupta, "Modular design and modular program for high gradient quadrupoles," *IEEE Trans. Appl. Supercond.*, vol. 17, no. 2, pp. 1273–1276, Jun. 2007.

[3] L. Hand and W. Panofsky, "Magnetic quadrupole with rectangular aperture," *Rev. Sci. Instrum.*, vol. 30, no. 10, pp. 927–930, 1959.

[4] V. V. Kashikhin, J. Strait, and A. V. Zlobin, "2nd generation LHC IR quadrupoles based on Nb_3Sn racetrack coils," in *Proc. Eur. Part. Accel. Conf.*, Lucerne, Switzerland, Jul. 2004, pp. 1774–1776.

[5] P. Ferracin *et al.*, "Development of a large aperture Nb_3Sn racetrack quadrupole magnet," *IEEE Trans. Appl. Supercond.*, vol. 15, no. 2, pp. 1132–1135, Jun. 2005.

[6] B. Parker, "Fast track actively shielded Nb_3Sn IR quadrupole R&D," Oct. 11, 2017. [Online]. Available: https://indico.bnl.gov/getFile.py/access?contribId=28&sessionId=5&resId=1&materialId=slides&confId=3492

[7] "eRHIC pre-conceptual design report," IPAC, Vancouver, BC, Canada, Tech. Rep. BNL 205809-2018-FORE, 2018.

[8] R. Rajput-Ghoshal, R. Fair, P. K. Ghoshal, E. Sun, C. Hutton, and M. Wiseman, "Preliminary design of the interaction region magnets for future electron-ion collider at Jefferson Lab," *IEEE Trans. Appl. Supercond.*, submitted for publication.

[9] M. Wiseman, C. Hutton, F. Lin, V. Morozov, and R. Rajput-Ghoshal, "Preliminary design of the interaction region beam transport systems for JLEIC," *IEEE Trans. Appl. Supercond.*, to be published.

[10] R. Gupta *et al.*, "Field compensation in electron-ion collider magnets with a passive superconducting shield," in *Proc. Appl. Supercond. Conf.*, 2018, Art. no. 2LPo2K-08.

[11] H. Felice *et al.*, "Magnetic and mechanical analysis of the HQ model quadrupole designs for LARP," *IEEE Trans. Appl. Supercond.*, vol. 18, no. 2, pp. 281–284, Jun. 2008.

[12] H. Oguro, S. Awaji, K. Watanabe, M. Sugimoto, and H. Tsubouchi, "Mechanical and superconducting properties of Nb_3Sn wires with Nb-rod-processed Cu Nb reinforcement," *Supercond. Sci. Technol.*, vol. 26, 2013, Art. no. 094002.